THE JOURNAL OF BIOLOGICAL CHEMISTRY Vol. 279, No. 13, Issue of March 26, pp. 12898–12908, 2004

Printed in U.S.A.

Identification and Characterization of EhCaBP2

A SECOND MEMBER OF THE CALCIUM-BINDING PROTEIN FAMILY OF THE PROTOZOAN PARASITE *ENTAMOEBA HISTOLYTICA**

Received for publication, May 6, 2003, and in revised form, December 28, 2003
Published, JBC Papers in Press, January 7, 2004, DOI 10.1074/jbc.M304716200

Paramita Chakrabarty‡§, Dhruv K. Sethi¶, Narendra Padhan‖, Kanwal J. Kaur¶, Dinakar M. Salunke¶, Sudha Bhattacharya‡, and Alok Bhattacharya‖**

From the ‡School of Environmental Sciences and the ‖School of Life Sciences, Jawaharlal Nehru University, New Delhi, India and the ¶National Institute of Immunology, New Delhi 110067, India

Entamoeba histolytica*, an early branching eukaryote, is the etiologic agent of amebiasis. Calcium plays a pivotal role in the pathogenesis of amebiasis by modulating the cytopathic properties of the parasite. However, the mechanistic role of Ca^{2+} and calcium-binding proteins in the pathogenesis of *E. histolytica* remains poorly understood. We had previously characterized a novel calcium-binding protein (EhCaBP1) from *E. histolytica*. Here, we report the identification and partial characterization of an isoform of this protein, EhCaBP2. Both EhCaBPs have four canonical EF-hand Ca^{2+} binding domains. The two isoforms are encoded by genes of the same size (402 bp). Comparison between the two genes showed an overall identity of 79% at the nucleotide sequence level. This identity dropped to 40% in the 75-nucleotide central linker region between the second and third Ca^{2+} binding domains. Both of these genes are single copy, as revealed by Southern hybridization. Analysis of the available *E. histolytica* genome sequence data suggested that the two genes are non-allelic. Homology-based structural modeling showed that the major differences between the two EhCaBPs lie in the central linker region, normally involved in binding target molecules. A number of studies indicated that EhCaBP1 and EhCaBP2 are functionally different. They bind different sets of *E. histolytica* proteins in a Ca^{2+}-dependent manner. Activation of endogenous kinase was also found to be unique for the two proteins and the Ca^{2+} concentration required for their optimal functionality was also different. In addition, a 12-mer peptide was identified from a random peptide library that could differentially bind the two proteins. Our data suggest that EhCaBP2 is a new member of a class of *E. histolytica* calcium-binding proteins involved in a novel calcium signal transduction pathway.

Ca^{2+} is a ubiquitous second messenger involved in signal transduction processes in eukaryotes (1). Intracellular Ca^{2+} gradients initiate a number of cellular processes including cell migration, exocytosis, activation of killer lymphocyte cells, cellular secretion, transcellular ion transport, neurotransmitter release, and gap junction regulation (2). These processes are essentially mediated by a variety of Ca^{2+}-binding proteins (CaBPs),[1] which are involved in binding Ca^{2+} and transducing the signal through downstream effectors. Calmodulin (CaM), a four EF-hand, highly conserved CaBP has been found in almost all eukaryotic cells and has been implicated in a large number of cellular processes (for review, see Ref. 3).

Ca^{2+} signaling also plays a crucial role in pathogenesis of many protozoan parasites (4). In *Plasmodium*, the expression of CaM has been shown to be stage-specific and is involved in erythrocyte invasion as well as schizont maturation (5). Chelation of Ca^{2+} can prevent hepatocyte invasion by merozoites (6). Ca^{2+} is also involved in invasion of host cells by trypanosomatids (7). Treatments that decrease or increase cytoplasmic Ca^{2+} modify *Trypanosoma cruzi* infectivity (8). Besides, Ca^{2+} also regulates various other cellular processes, such as apoptosis, loss of motility, environmental sensing, and excystation (9, 10). In the protozoan parasite *Entamoeba histolytica*, the causative agent of amebiasis, Ca^{2+} is reported to be involved in its pathophysiology by initiating the amebic cytolytic activity (for a recent review, see Ref. 11). Amebic cytolytic activity could be blocked by Ca^{2+} channel blockers, or by treatment with EGTA (12), whereas stimulation of amebic PKC activity with phorbol esters enhanced lysis of target epithelial cells (13). Changes in the Ca^{2+} profile were also related to the cell cycle and the developmental stages of the parasite *i.e.* the cyst or the trophozoite stage (14). Furthermore, extracellular Ca^{2+}, amebic intracellular Ca^{2+} flux, bepridil-sensitive Ca^{2+} channels and a putative CaM-dependent signal transduction pathway have been implicated in the growth and encystation of *Entamoeba* (15). Ca^{2+} is thus speculated to play a direct role in precipitating the cytopathic effects of *E. histolytica*.

A number of CaBPs have been identified in *E. histolytica* (4). Among these are two related EF-hand-containing proteins, grainin 1 and 2, which are localized in intracellular granules (16). They may be involved in phagocytosis, control of endocytotic pathways and Ca^{2+}-dependent granular discharge. Another protein, URE3-BP, was shown to have a transcription regulatory function with Ca^{2+}-dependent DNA binding properties (17, 18). CaM-dependent secretion of collagenases from electron dense granules has been demonstrated using *Entamoeba* lysate but a direct evidence for the presence of CaM is still lacking (19, 20). We had previously characterized a CaBP (EhCaBP1) from *E. histolytica* (21, 22). EhCaBP1 has 134 amino acid residues with

* This work was supported in part by grants from the Department of Biotechnology and Department of Science & Technology, Government of India. The costs of publication of this article were defrayed in part by the payment of page charges. This article must therefore be hereby marked "*advertisement*" in accordance with 18 U.S.C. Section 1734 solely to indicate this fact.

The nucleotide sequence(s) reported in this paper has been submitted to the GenBank™/EBI Data Bank with accession number(s) AY515693.

§ Recipient of a University Grants Commission predoctoral fellowship.

** To whom correspondence should be addressed: School of Life Sciences, Jawaharlal Nehru University, New Mehrauli Road, New Delhi-110067, India. Tel.: 91-11-26704516; Fax: 91-11-26165886; E-mail: alok0200@mail.jnu.ac.in.

[1] The abbreviations used are: CaBP, calcium-binding protein; CaM, calmodulin; nt, nucleotide; MD, molecular dynamics; ORF, open reading frame; pC112, synthetic peptide C112; pC61, synthetic peptide C61; RT-PCR, reverse transcription-PCR; TMB, 3,3′,4,4′-tetramethylbenzidine.

four canonical EF-hand Ca^{2+} binding domains. Though this protein has some structural similarity with CaM, it is functionally quite distinct (23). Inducible expression of EhCaBP1 antisense RNA demonstrated its role in cellular proliferation (24, 25).

Structural studies on EhCaBP1 have revealed an organization similar to CaM, having two independent globular domains connected by a flexible linker. It consists of four canonical EF-hands, a pair each in the N- and C-terminal domains. The Ca^{2+} binding loops in the protein consist of 12 contiguous residues flanked by two helices, which are, oriented nearly perpendicular to each other, a feature shared by other members of the family of EF-hand proteins (26). EhCaBP1 is structurally related to CaM and Troponin C (TnC) despite low sequence homology with these proteins. The major differences in the structure of EhCaBP1 with respect to CaM and TnC are in the Ca^{2+} binding loops, interhelical angles and exposed hydrophobic surface. These differences have led to a more open conformation for the Ca^{2+} binding loops in the C-terminal domain of EhCaBP1 compared with the ones in the N-terminal domain and higher solvent exposure of the hydrophobic residues (27, 28). In EhCaBP1, the linker region exhibits a large structural flexibility, leading to an ill-defined orientation of the two domains (N- and C-terminal) with respect to each other. These structural features make EhCaBP1 functionally distinct from other CaM-like Ca^{2+}-binding proteins. In this study, we report the identification and partial characterization of EhCaBP2, a paralog of EhCaBP1, and show that these two proteins are functionally distinct.

EXPERIMENTAL PROCEDURES

Strains and Cell Growth—E. histolytica strain HM1:IMSS was maintained at 36 °C in TYI-S-33 medium with appropriate antibiotics (29).

Southern and Northern Hybridization—Total DNA was purified from late-log phase grown cells, as described earlier (30). Genomic DNA, digested with appropriate restriction enzymes and separated on an agarose gel, was transferred to nylon membranes. Southern blots were hybridized in a solution containing 1% SDS, 1 M NaCl, and 3×10^5 cpm ml^{-1} of DNA probe at 65 °C for 16 h. Blots were washed according to the manufacturer's instructions and exposed for autoradiography. Radioactive DNA probes were prepared using the NEBlot random priming kit (NEB).

Total RNA was purified using TriPure reagent (Roche Applied Science) according to the manufacturers' instructions. RNA samples (30 μg) were denatured by incubating with 6 M deionized glyoxal, 50% (v/v) Me_2SO and 1× gel running buffer (12 mM Tris-HCl, 6 mM sodium acetate, and 0.3 M EDTA, pH 7.0) at 50 °C and electrophoresed in a 1.2% (w/v) Tris acetate-EDTA (TAE) agarose gel. After electrophoresis, the gel was blotted on to a GeneScreen plus (GS+) nylon membrane (NEN), and hybridization was carried out at 42 °C in 50% formamide-containing hybridization buffer according to the manufacturer's instructions.

Polymerase Chain Reaction—Primers to amplify the EhCaBP2 ORF were designed based on the *Entamoeba* GSS sequence data base. The primers used (Primer 1: 5′-GGGAAACATATGTCATTACAAAAGAT-T-3′ and Primer 2: 5′-GGGAAAGGATCCTTAAAGATTGAATGC-3′) were obtained from Microsynth, Switzerland. PCR was performed with 400 ng of *E. histolytica* genomic DNA. The conditions were: 92 °C, 5 min; 36 °C, 1 min; 70 °C, 1 min (5 cycles); 92 °C, 1 min; 56 °C, 1 min; 70 °C, 1 min (25 cycles). The PCR products were cloned in pGEMTeasy vector (Promega) and subsequently in pET30a vector (Novagen) for expression in *E. coli* BL21 (DE3) cells.

The primer set 3–4 was used to amplify reverse-transcribed products obtained from total HM1:IMSS RNA (primer 3: 5′-GTTCAAGTATAA-ATTCATTACAAAAGATT-3′; Primer 4: 5′-GTTCTTTAACAGCAGCTG-CA-3′). The conditions used were 92 °C, 1 min; 48 °C, 1 min; 70 °C, 1 min (30 cycles).

Expression and Purification of Recombinant EhCaBP2 in E. coli—The purification of recombinant EhCaBP2 was carried out essentially as described earlier (22). Induced bacterial cells were resuspended in 50 mM Tris, pH 7.5 and 2 mM EGTA and lysed by freeze-thaw followed by sonication. Heat treatment of the lysed cells was carried out by incubation in a boiling water bath for 3 min followed by separation of heat-precipitable *E. coli* cellular proteins. The supernatant, containing recombinant EhCaBP2, was purified using ion-exchange chromatography employing methods described earlier (22). The Ca^{2+}-free EhCaBP2 was prepared with the help of Chelex 100 as described (31).

Affinity Purification of EhCaBP-binding Proteins—The EhCaBP-binding proteins were purified using the respective EhCaBP-Sepharose affinity chromatography as described before (23). The soluble cytoplasmic fraction was first diluted in Buffer C (20 mM Tris-Cl, pH 7.5, 1 mM imidazole, 1 mM magnesium acetate, 1 mM $CaCl_2$, 2 mM β-mercaptoethanol) and passed through EhCaBP-Sepharose 4B column (4–6 mg of protein per ml of bed volume). Unbound proteins were washed with 10 bed volumes of Buffer C. The bound proteins were eluted with Buffer D (same as Buffer C except that $CaCl_2$ is replaced with 2 mM EGTA) as 1-ml fractions. The chromatographic steps were carried out at 4 °C. The eluates were dialyzed against water and then concentrated by centrifugal evaporation.

Laser Ionization Time of Flight Mass Spectrometry (MALDI-TOF)—MALDI-TOF spectrometry was used to analyze EhCaBP-binding proteins. The matrix was prepared using sinapinic acid in 30% (v/v) acetonitrile, and 0.33% trichloroacetic acid, and the samples were analyzed by a MALDI-TOF spectrometer (Kratos PCKOMPACT SEQ model). The mass calibration was carried out using the MS-CAL1 mass calibration kit for MALDI-MS (Sigma).

In Vitro Kinase Assay—Total *Entamoeba* cell extract was prepared and the activity of Ca^{2+}-dependent kinases was estimated according to Chandok and Sopory (30). The reaction mixture contained 30 mM HEPES, pH 7.5, 5 mM $MgCl_2$, 40 μg of histone (Type IIIS, Sigma), 30 μg of *E. histolytica* cell extract, protease inhibitor mixture, $CaCl_2$ or EGTA, and 100 pmol of peptide where indicated. The reaction volume was adjusted to 50 μl. The reaction was initiated by adding 100 μM [γ-^{32}P]rATP (specific activity 5000 Ci/mmol, Amersham Biosciences) and allowed to proceed at 30 °C for 10 min. The reaction was terminated by adding 10% trichloroacetic acid, which precipitated total protein in the reaction mixture. The pellet was washed with diethyl ether/ethanol (1:1) mixture and after drying the pellet, and spotting the rehydrated pellet on GF/C paper, the amount of radioactivity was determined in a scintillation counter. For visualization of phosphorylated products, the reaction mixture after termination was separated in a 10% SDS-PAGE. The fluorographed gels were dried and exposed to an x-ray film. In competition experiments involving peptides, reactions were performed under identical conditions using *E. histolytica* total cell lysate preincubated with indicated amounts of peptide(s).

Ca^{2+}-dependent Phage ELISA—Phages were prepared according to standard procedures and phage ELISA assays were performed essentially as described earlier (32). However, certain changes were introduced to ensure that the phage binding was Ca^{2+}-dependent. The phages were allowed to bind to the EhCaBPs in the presence of 2 mM $CaCl_2$. The plates were washed in TBST containing either 2 mM $CaCl_2$ or 4 mM EGTA, and the bound phages were detected using horseradish peroxidase-labeled anti-M13 monoclonal antibody (Amersham Biosciences; 1:3000 dilution) with TMB substrate (Amersham Biosciences) at 410 nm.

Surface Plasmon Resonance Analysis—Binding kinetics of phages to protein was determined using IAsys Auto$^+$ (Affinity sensor). Amplified phages (10^{11} pfu/ml) from a 20-ml culture were precipitated and dissolved in 50 μl of phosphate-buffered saline, pH 7.4. Phages were biotinylated using established protocols (33). Biotinylated phages were immobilized onto streptavidin bound on a biotin-coated surface. For determination of association rate constants, EhCaBPs (25–400 μM) in the binding buffer (10 mM Tris, pH 7.5, 150 mM NaCl, 2 mM $CaCl_2$) were used. Following analyte binding, dissociation rate constants were measured by replacing the sample with binding buffer. The surface was regenerated with the regeneration buffer (10 mM Tris, pH 7.5, 150 mM NaCl, 4 mM EGTA). Kinetics of the interaction of EhCaBPs with phages were analyzed by non-linear regression using FASTfit software package supplied with IAsys instrument.

Sequence Analysis—Preliminary sequence data for *E. histolytica* is deposited regularly into the GSS division of GenBank™ and was used for this analysis. The sequencing effort is part of the International *Entamoeba* Genome Sequencing Project and is supported by award from the National Institute of Allergy and Infectious Diseases, National Institutes of Health.

The *Entamoeba* genome sequence data base from the Sanger Centre (www.sanger.ac.uk) supported by the Welcome trust was also used. BLAST searches (NCBI: www.ncbi.nlm.nih.gov/BLAST) were used for finding homologues of EhCaBPs. ClustalW (EMBL: www.ebi.ac.uk) was used for alignment of multiple sequences.

Molecular Modeling—Molecular modeling was carried out using the Modeler (34) interface of INSIGHTII (Molecular Simulations Inc.) The model was built on the basis of the NMR solution structure (1JFK) of the Ca^{2+}-bound form of EhCaBP1 (28). The constructed model was

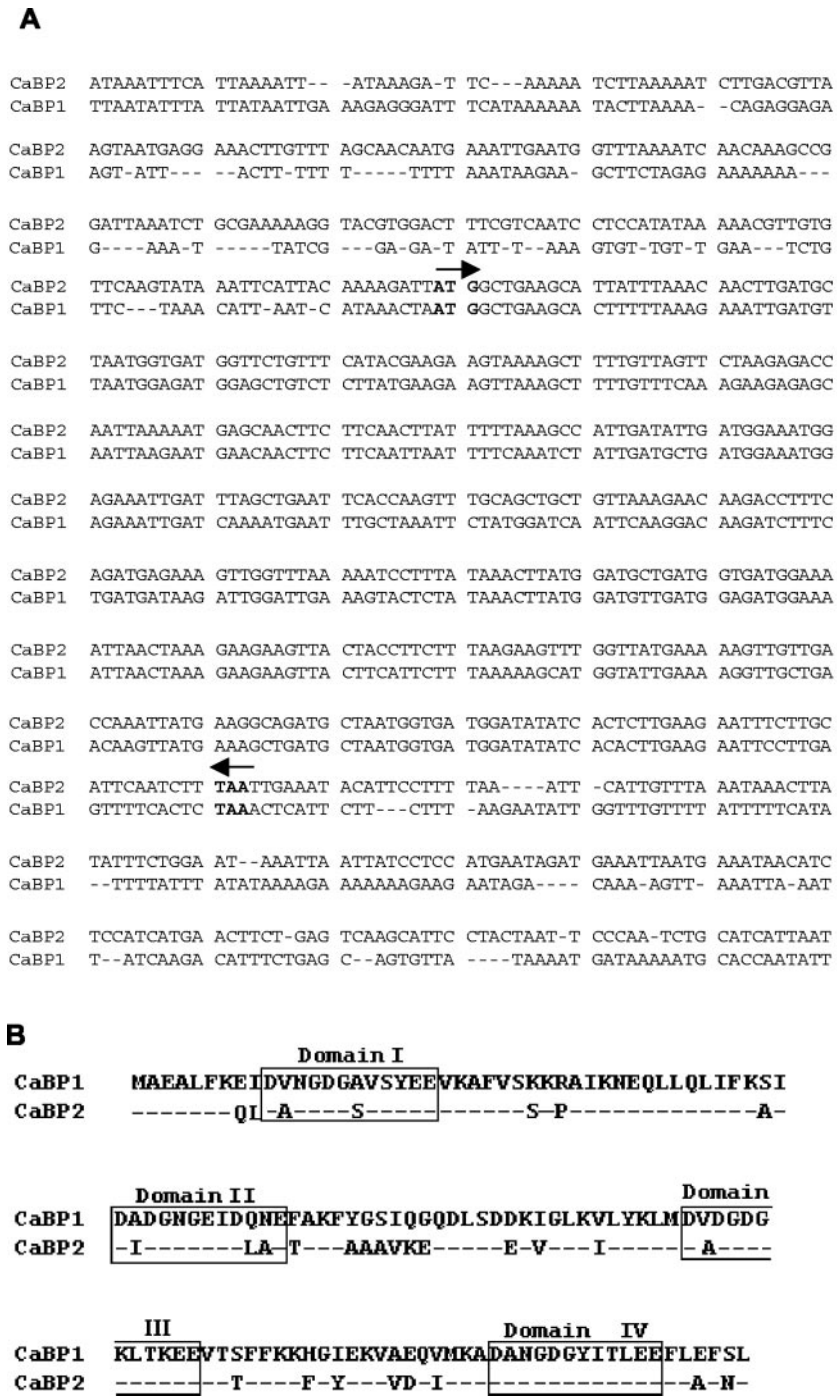

FIG. 1. **Sequence analysis of EhCaBP2.** *Panel A*, alignment of nucleotide sequences of EhCaBP1 (Sanger contig 3894) and EhCaBP2 (Sanger contig 4494) using ClustalW. The beginning and the end of the ORFs are marked by *arrows*. The start (ATG) and the stop (TAA) codons are highlighted. *Dashed lines* indicate introduction of gaps to maintain optimal alignment. *Panel B*, alignment of amino acid sequences of EhCaBP1 and EhCaBP2. The *dashed lines* represent identical amino acids and the canonical EF-hand domains (I to IV) are marked in *boxes*.

minimized initially with full backbone constraints, which were gradually relaxed as the minimization proceeded. The final model was validated by PROCHECK (35).

Molecular dynamics simulation was carried out to explore the conformational variation existing in the flexible linker region between the two domains in EhCaBP1 and EhCaBP2. 10 ps of equilibration at 300 K were followed by 100 ps of molecular dynamics (MD) simulation. The MD simulation was carried out for the 13 residues of the linker region with maximum variability, while the rest of the structure was constrained. RMSD for 10 representative MD-derived structures of the linker region (residues 55–67) was found to be 0.32 Å suggesting no significant variation from the average structure.

Circular Dichroism Spectroscopy—CD measurements were performed using a Jasco-810 spectropolarimeter. Each spectrum was measured in the far-UV region (200–270 nm) and was an average of five scans. Scans were done at a protein concentration of 1 μM using a cuvette of pathlength 1 cm. Percentage helical content was calculated using the method described by Barrow *et al.* (36).

Miscellaneous Methods—The concentration of protein in a sample was estimated by bicinchoninic acid assay using bovine serum albumin (BSA) as a standard (37). Sodium dodecyl sulfate polyacrylamide gel electrophoresis (SDS-PAGE) analysis was carried out in 10 or 14% acrylamide gels, as indicated, under reducing conditions according to Laemmli (38). Following electrophoresis, the gels were subjected to fluorography as described by Laskey and Mills (39). Peptides (Peptide C61, pC61:GAWYPREASTAS; Peptide C112, pC112: SMNLQTPGYKDG, Control 12-mer peptide, p12: YIPQPRPPHPGL) were synthesized. Peptides were desalted and purified by reverse-phase HPLC using a C_{18} column and their amino acid sequence confirmed.

RESULTS

A Second E. histolytica Calcium-binding Protein (EhCaBP2)

Our laboratory had previously characterized a calcium-binding protein, EhCaBP, from *E. histolytica* (21). A search for the

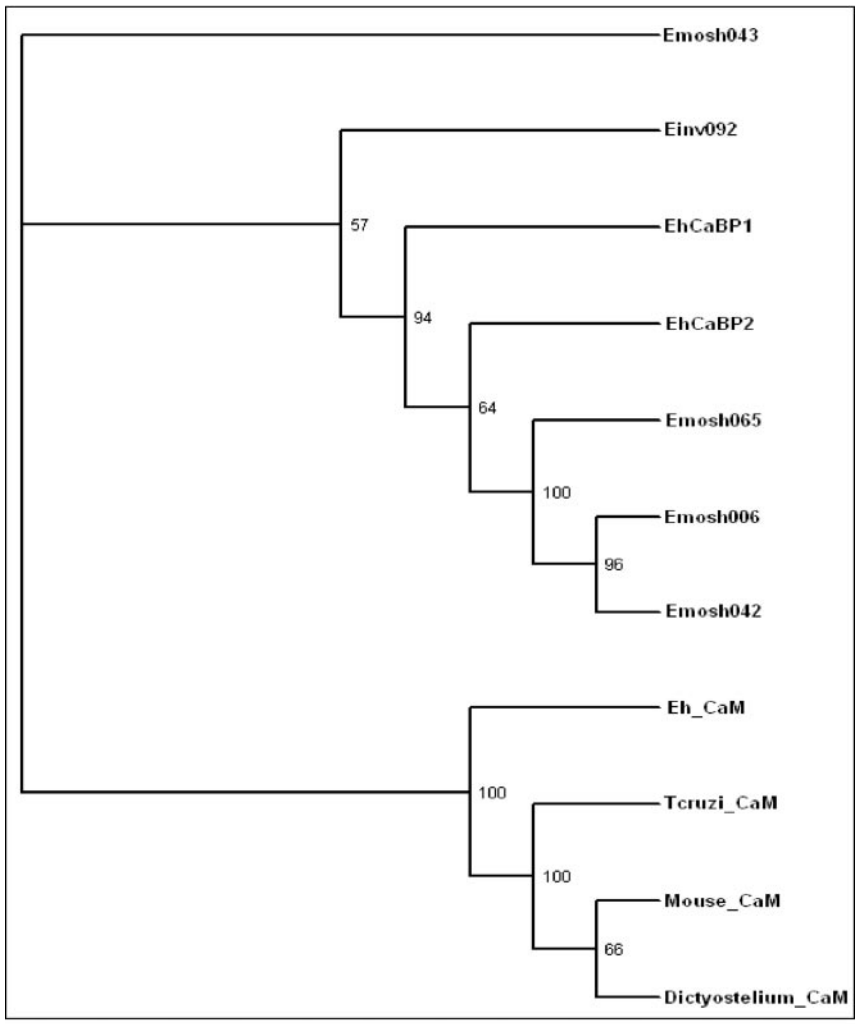

FIG. 2. **Phylogenetic analysis of EhCaBPs.** The tree was constructed on the basis of the alignment generated using ClustalW with manual editing. Dayhoff's amino acid matrix program was used for generating the tree. Bootstrap values are indicated at each branch point.

presence of EhCaBP homologs in the *E. histolytica* genome sequence data base at NCBI revealed (in addition to an entry with complete match with EhCaBP) a sequence that showed a very high score and low p value (score = 163; $p = 4e^{-38}$) using BLAST. The identified sequence was then used to find a contig that carried the entire coding region, from the genome data base at the Sanger Centre, UK (contig 4494). The second gene was designated as EhCaBP2 whereas the original gene was renamed EhCaBP1.

The overall identity at the nucleotide level between EhCaBP2 and EhCaBP1 was 79% (Fig. 1*A*). Of the 80 nucleotides that differed in the two genes, 28 were in the third codon position, leaving the encoded amino acids unchanged. The conceptual translation product of EhCaBP2 was compared with EhCaBP1 and the alignment of the two sequences is shown in Fig. 1*B*. The amino acid sequences of the two proteins showed an identity of 78%. Both the proteins have four typical EF-hand Ca^{2+} binding domains. The level of similarity between the two proteins varied along the length of the sequence. The maximum identity was observed in the Ca^{2+} binding domains with a total of 6 amino acid substitutions (Fig. 1*B*). The minimum identity was seen in the 27 amino acid central linker region between Ca^{2+} binding domains 2 and 3, which had 10 substitutions. The sequence comparison shows that the overall structure of both the proteins is similar, but the two may perform different functions due to variations in the central linker.

The nucleotide sequences upstream and downstream of the ORF of EhCaBP1 and EhCaBP2 showed no significant sequence identity (Fig. 1*A*). In addition, genes present in the vicinity of each EhCaBP were different. The putative ORF located upstream of EhCaBP1 was the human homolog of AMP-deaminase (Score = 72, $p = 2e^{-12}$) whereas the ORF upstream of EhCaBP2 had similarity to myosin heavy chain (Score = 56, $p = 3e^{-7}$). Therefore, these two EhCaBP genes are unlikely to be allelic copies.

Currently, genomic sequences from different species of *Entamoeba* are being deposited in the GSS databases maintained at the Sanger Centre. The putative coding regions of several EhCaBP-like sequences were identified from this data base using standard bioinformatics tools. A CaM-like protein displaying 50–78% identity to other calmodulins was also identified in this data base (contig 5693). A phylogenetic analysis of the EhCaBPs and related orthologs and paralogs and different calmodulins revealed that all *Entamoeba* CaBPs are distinctly different from CaMs including that from *E. histolytica* (Fig. 2). A close examination of the tree revealed minor differences among the CaBPs from different *Entamoeba* species. Among the *Entamoeba* CaBP orthologs, *E. invadens* displayed the maximum divergence. None of the EhCaBP-like *Entamoeba* CaBPs is close to CaM as the two segregate out in different clusters. The groupings were well supported by high bootstrap values. Interestingly, none of the sequences were found more than once in the data base, which may imply all of these isoforms may not be duplicated pseudogenes. From this analysis, it appears that EhCaBP1 and EhCaBP2 are paralogs of each other as they branched out separately.

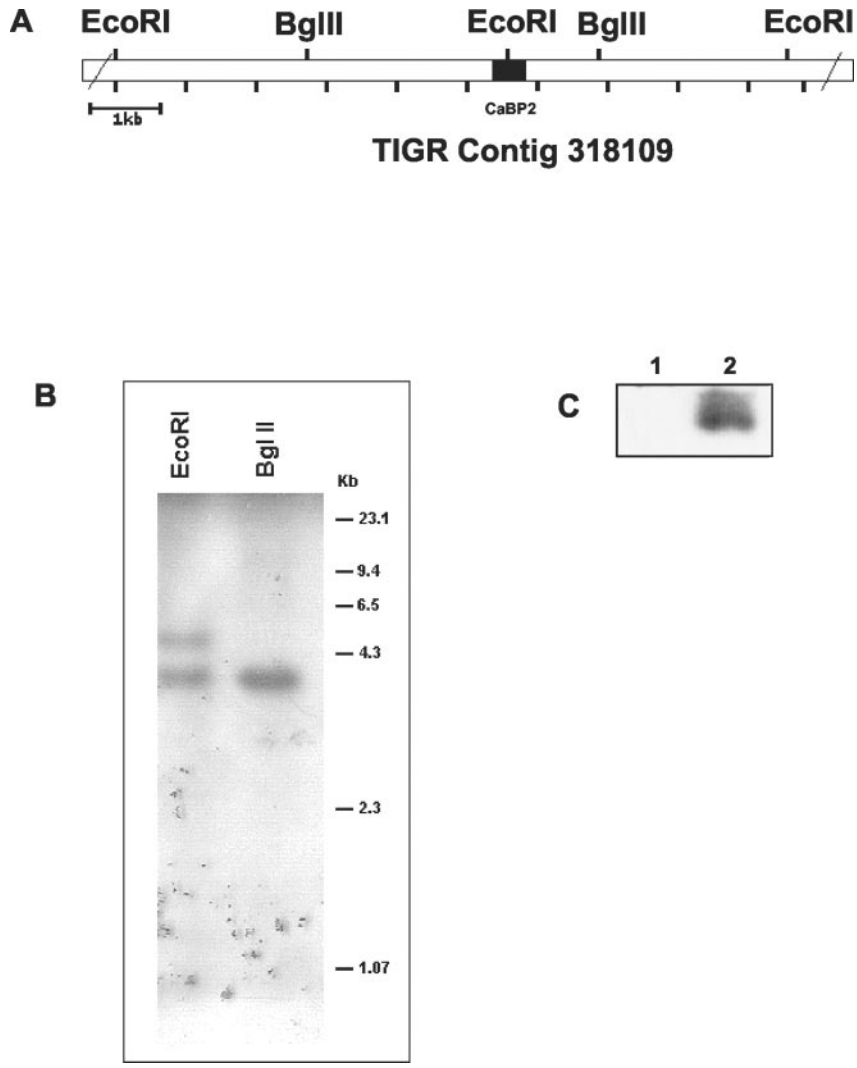

FIG. 3. **Southern blot analysis of EhCaBP2.** *Panel A*, schematic representation of the positions of EcoRI and BglII sites located on contig 318109 (TIGR data base). The position of the EhCaBP2 ORF is marked by a *closed box*. The scale (1 kb) is indicated. *Panel B*, 1 μg of genomic DNA from *E. histolytica* HM-1:IMSS was digested with indicated restriction enzymes, separated in a 0.8% agarose gel at 4 V/cm and hybridized with EhCaBP2 ORF as described under "Experimental Procedures." *Panel C*, Southern hybridization of cloned EhCaBPs with the radiolabeled EhCaBP2 probe was carried out as described for *panel B*. The plasmid DNAs were first separated in 0.8% agarose gel before transfer and hybridization. *Lane 1*, EhCaBP1; *lane 2*, EhCaBP2.

Copy Number of EhCaBP2

To determine the copy number of EhCaBP2, *E. histolytica* genomic DNA was digested with the restriction enzymes BglII and EcoRI. From the nucleotide sequence of EhCaBP2, it was determined that BglII does not have a site in the coding region whereas EcoRI has a single site. Genomic DNA digested with these enzymes was blotted and hybridized with EhCaBP2 probe. The EcoRI-digested DNA hybridized to two bands of sizes 6.0 kb and 4.36 kb while BglII-digested DNA hybridized with a single band of 4.36 kb (Fig 3*B*). Under the conditions of hybridization, the EhCaBP2 coding region probe specifically hybridized to EhCaBP2 DNA and not EhCaBP1 DNA (Fig. 3*C*). The sizes of bands obtained by Southern hybridization matched very well with the expected sizes from nucleotide sequence of the 18-kb TIGR contig 318109, which contains the EhCaBP2 ORF (Fig. 3*A*). The Southern data show that EhCaBP2 is a single copy gene.

Expression of EhCaBP2 in E. histolytica HM-1:IMSS

Expression of EhCaBP2 was checked in order to rule out the possibility that it could be a pseudogene. A search of the data base revealed an EST (accession no. AB002775) with 100% identity with EhCaBP2 at the nucleotide level, suggesting that this gene may be expressed in *E. histolytica* trophozoites (40). The presence of EhCaBP2 transcript was confirmed using both RT-PCR and Northern hybridization. EhCaBP2-specific primers were designed from the regions that showed maximum variability with respect to EhCaBP1 (marked in Fig 4*A*, *top panel*). The specificity of the primers was checked by a PCR reaction using cloned EhCaBP1 and EhCaBP2 genes as templates (Fig. 4*A*, *lanes 1* and *2*). A band of 225 bp was detected after RT-PCR of RNA isolated from axenic trophozoites (Fig. 4*A*, *lane 3*). In the absence of reverse transcriptase (Fig. 4*A*, *lane 4*), no such amplification was detected, showing the absence of any contaminating DNA.

In addition, Northern hybridization of total HM1:IMSS RNA, carried out at high stringency as described under "Experimental Procedures," revealed a single species of RNA transcript of 0.57 kb (Fig. 4*B*). Under the conditions used, the EhCaBP2 probe did not hybridize with EhCaBP1 (Fig. 4*B*, *inset a*). The data indicate that EhCaBP2 is expressed in *E. histolytica.*

Ca^{2+} Binding Properties of Recombinant EhCaBP2

The EhCaBP2 ORF (402 bp) from strain HM-1:IMSS was amplified using primers 1–2 designed from the GSS entry AZ542766. The PCR-amplified product was cloned into the expression vector pET30a as described under "Experimental Procedures." The recombinant protein was purified from the induced bacterial lysate (data not shown) using a method developed for purification of recombinant EhCaBP1 (22). The Ca^{2+}-free form of the protein was used for all experiments involving Ca^{2+} binding which was evaluated by CD spectroscopy. CD studies were carried out on both holo and apo forms of EhCaBP2. The CD profiles of the two protein forms showed

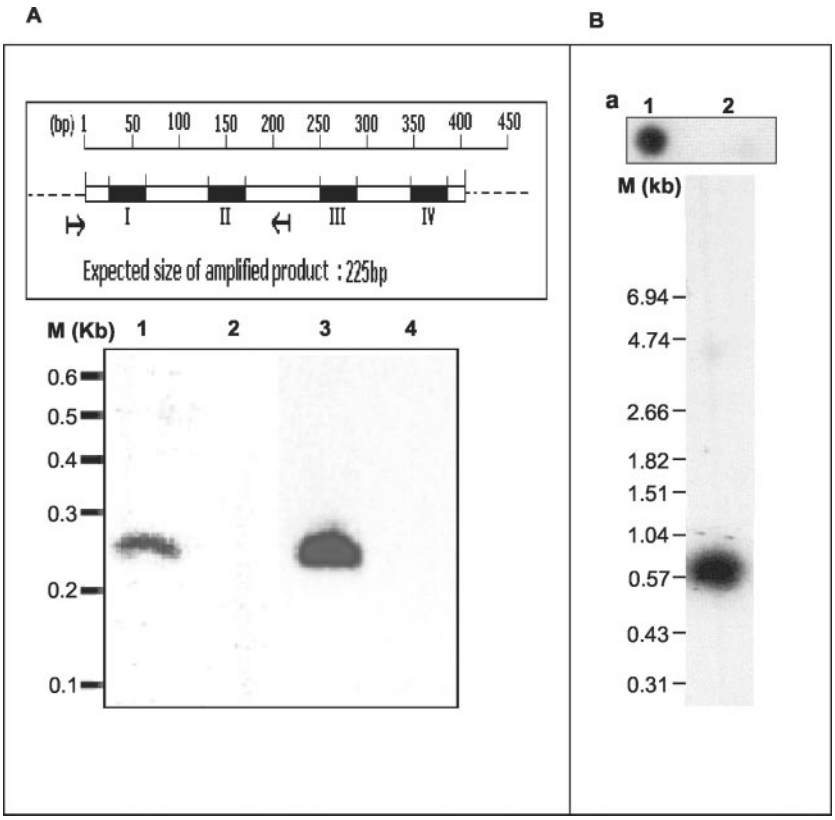

FIG. 4. **Expression of EhCaBP2 RNA in *E. histolytica*.** *Panel A*, amplification of EhCaBP2 RNA by RT-PCR. The location of the primers is indicated with *arrows* at the top of the figure. The positions of the calcium binding domains are marked I-IV in this scheme. The specificity of the primers for EhCaBP2 was checked by PCR amplification of EhCaBP1 and EhCaBP2-containing plasmid templates. The PCR products were electrophoresed in 1.2% agarose gel at 4 V/cm. *Lane 1*, EhCaBP2 plasmid DNA; *lane 2*, EhCaBP1 plasmid DNA; *lane 3*, total HM1:IMSS RNA and *lane 4*, same as *lane 3* except no reverse transcriptase was added. *Panel B*, Northern blot analysis of EhCaBP2. 30 μg of purified total RNA was separated in a 1.2% denaturing formaldehyde agarose gel and transferred onto a nylon membrane. The blot was hybridized with a radiolabeled EhCaBP2 coding region probe as described under "Experimental Procedures." *Inset a*, the probe was also hybridized with plasmid DNA (5 ng) containing cloned insert under the same condition. *1*, EhCaBP2 and *2*, EhCaBP1.

significant differences, which could be directly attributed to conformational differences. Thus, a distinct conformational change, evident in terms of the increase in the helical content, was observed in the holo-EhCaBP2 as compared with the apoprotein (Fig. 5). The helical content in the case of holo-EhCaBP2 was about 56% and that in the case of the apoprotein was found to be 35%. A similar trend was also reported earlier with regard to the helical contents of the apo- and the holo-EhCaBP1 (31).

Structural Model of EhCaBP2

A model for EhCaBP2 was built using methods described under "Experimental Procedures." (34). A comparative study of the two proteins was done at the primary as well as the tertiary level. The high sequence homology of the two proteins, EhCaBP1 and EhCaBP2 was reflected in similar structural topologies for the two proteins namely, the basic tertiary structure of two globular domains with the four well-conserved EF-hands (Fig. 6*a*). The Ca^{2+} binding domains show high degree of structural similarity between the two EhCaBPs. Residues responsible for Ca^{2+} binding in EhCaBP1 were mapped using CONTACT (CCP4 Suite); only one residue, Ala^{16}, in the Ca^{2+} binding site of EhCaBP1 was found to be mutated to Ser^{16} in EhCaBP2. However, significant differences were seen in the flexible linker region. A reduction in helicity, leading to a more compact structure in the EhCaBP2 linker region was evident, with its helix being four residues shorter than that of EhCaBP1. The resultant structural compaction might be due to the absence of several bulky side chains in the linker region of EhCaBP2. Charge differences also exist between EhCaBP1 and EhCaBP2 (Fig. 6, *b–e*); the surface of EhCaBP1 is more positively charged compared with that of EhCaBP2. Due to the compact packing within the EhCaBP2 linker region (Fig. 6*a*) K74, which is a major component of a positively charged patch in EhCaBP1 gets buried in EhCaBP2 by E67 (Gly^{67} in EhCaBP1). Lys^{28} and Arg^{30}, which are located on the surface of

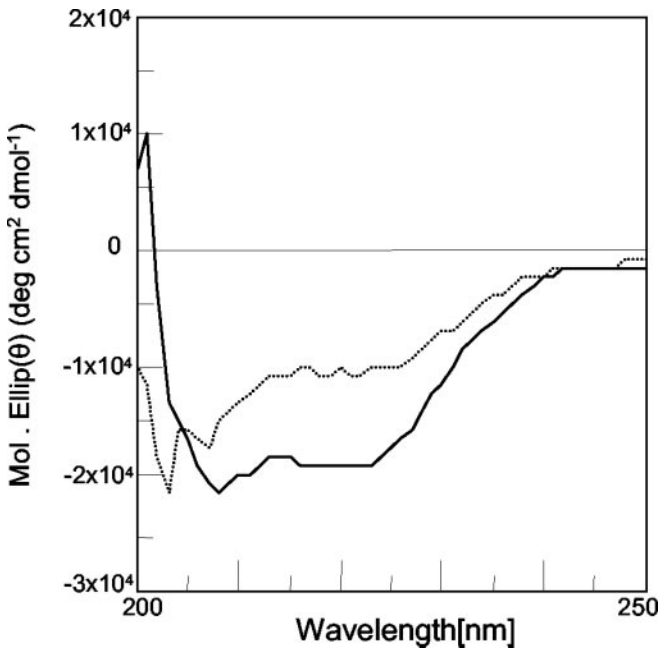

FIG. 5. **CD Spectrum of EhCaBP2.** The CD profile of EhCaBP2 was obtained in aqueous buffer. The *thick continuous line* represents the profile for the holo and *dotted discontinuous line* is that of the calcium-free apo protein.

EhCaBP1, contributing to a significant positively charged patch, are changed to Ser^{28} and Pro^{30} in EhCaBP2 leading to significant reduction in the positive charge on the surface. The CD spectra also showed that the Ca^{2+}-bound form of EhCaBP2 exists in a largely helical conformation (Fig. 5).

Functional Analysis of EhCaBP2

Analysis of Binding Proteins—The purified EhCaBP1- and EhCaBP2-binding proteins were analyzed by MALDI/TOF

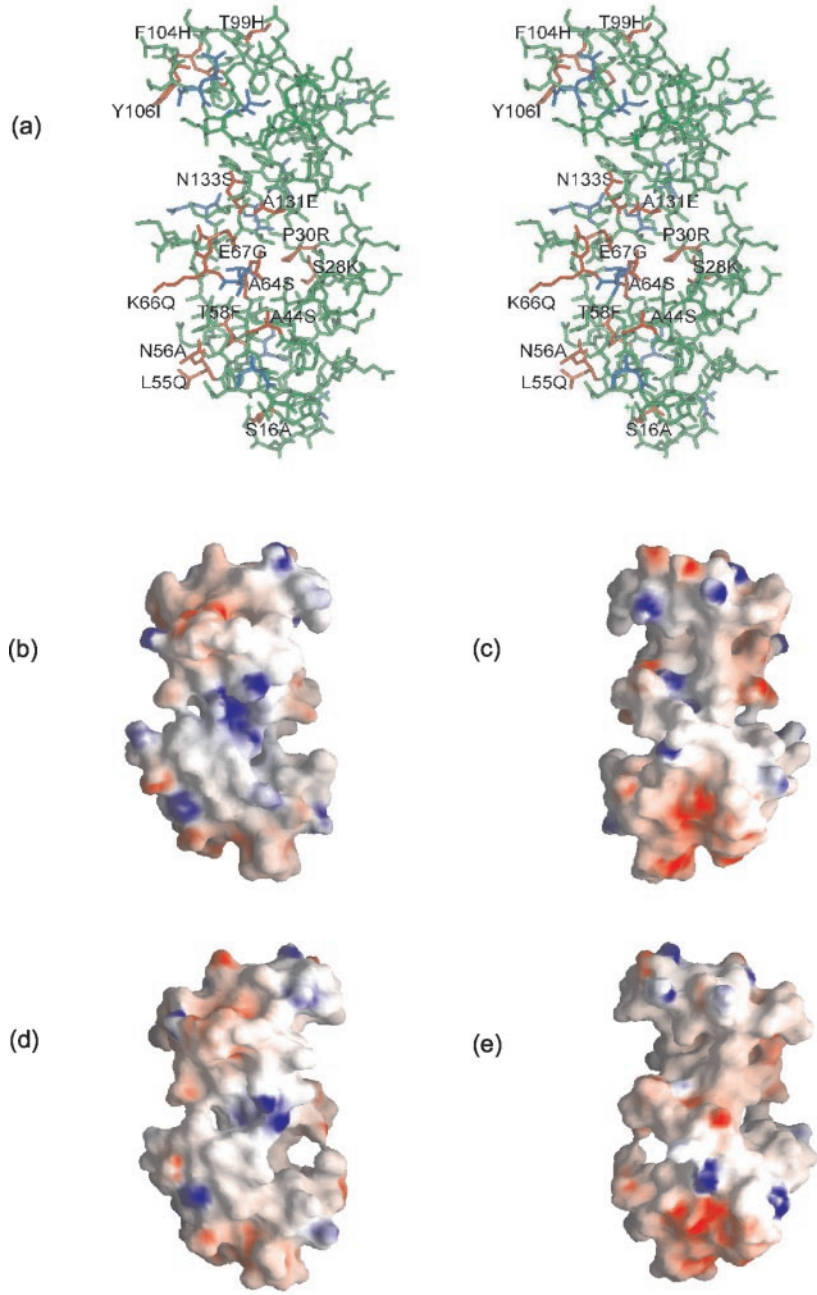

FIG. 6. **Comparative modeling of EhCaBP2.** Stereoscopic representation showing residues mutated in CaBP2 with respect to CaBP1. *Panel a*, unrelated amino acid replacements are indicated in *red*. Mutations to similar amino acids are shown in *blue*. The surface features of EhCaBP1, front (*panel b*) and back view (*panel c*) have been compared with those of EhCaBP2, front (*panel d*) and back view (*panel e*). The solvent accessible surfaces of the proteins have been color coded according to charge: *red negative* and *blue positive*.

mass spectrometer. The spectrum differed considerably for the two sets of binding proteins (Fig. 7). Whereas there was essentially a single major species of 95 kDa among the EhCaBP2-binding proteins, a number of polypeptides were observed among EhCaBP1-binding proteins. No common peak was observed in both the spectra suggesting that the two proteins bind different targets. Mass spectrometric pattern of binding proteins was found to be somewhat different from that obtained by SDS-PAGE analysis of [^{35}S]methionine-labeled binding proteins prepared in the same way (data not shown here). It may be due to uneven labeling of proteins with [^{35}S]methionine independent of size or relative amount or lack of effective separation at high molecular weight range in SDS-PAGE.

Activation of Endogenous Kinase—EhCaBP1 was shown to activate endogenous kinase(s) that may be an important component of the Ca^{2+}-signal transduction pathway mediated by this protein (23). The ability of EhCaBP2 to activate an endogenous kinase was similarly tested. The *in vitro* system for assaying kinase activity included *E. histolytica* cell lysate as the source of kinase, and histone as the substrate. The reaction was carried out in the presence of 10 and 100 μM Ca^{2+} with varying concentrations of EhCaBP2 (Fig. 8*B*). The two Ca^{2+} concentrations were chosen on the basis of our previous work where two Ca^{2+}-dependent kinase activities were found in the amebic lysate, with optimum activation at 10 and 100 μM added Ca^{2+} respectively (23). The data showed that, indeed, EhCaBP2 could also activate an endogenous kinase in the presence of 100 μM added Ca^{2+} and at 2 nM protein concentration. In contrast, EhCaBP1-dependent kinase activity was optimal at 10 μM added Ca^{2+} as reported earlier (Fig. 8*A*). Therefore, these two proteins differ in the Ca^{2+} concentrations required for optimal activity.

In order to identify the endogenous substrate of Ca^{2+}/EhCaBP2-dependent kinase, a phosphorylation assay was performed in the absence of any exogenous acceptor, and the products were separated by SDS-PAGE. The result was compared with that obtained with EhCaBP1 to see if the two

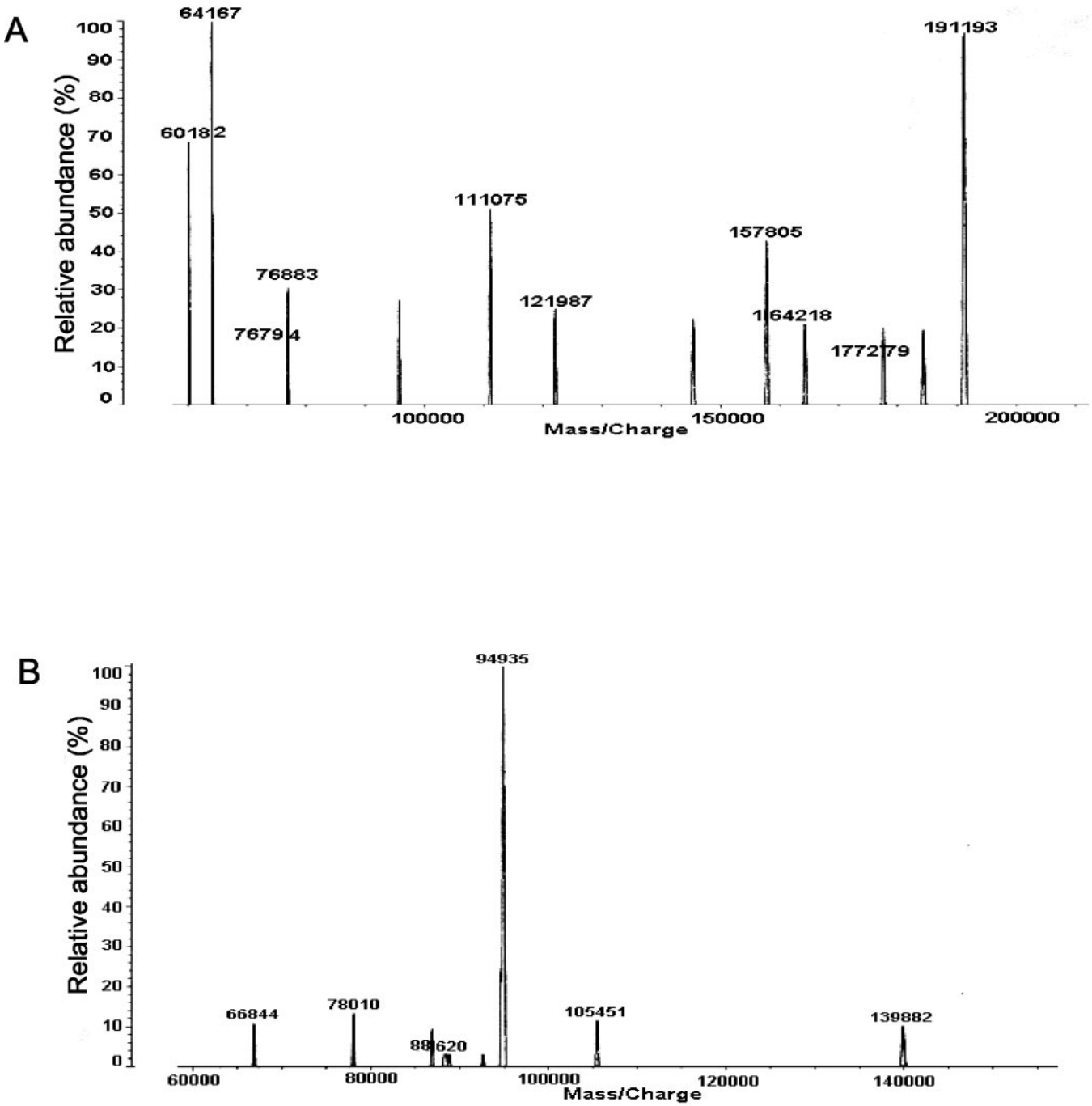

FIG. 7. **MALDI-TOF mass spectrometric analysis of EhCaBP-binding proteins.** The binding proteins were purified using affinity chromatography over respective EhCaBP-Sepharose matrix as described in the text. The proteins eluted in the presence of EGTA were dialyzed against water and then concentrated before mass spectrometric analysis. MALDI spectrum of EhCaBP1-binding proteins (*A*) and EhCaBP2-binding proteins (*B*).

proteins share the same substrate. Both these proteins were found to stimulate phosphorylation of a 47 kDa protein present in the cell-free lysate of *E. histolytica* (Fig. 8*C*). However, the extent of phosphorylation by EhCaBP2 was at least 20 times more than that by EhCaBP1 under identical experimental conditions (Fig. 8*C*). The relative ability of the two EhCaBP-dependent kinases to phosphorylate histone or endogenous polypeptide as substrates differed significantly and may be due to their relative affinities for the different substrates. The phosphorylated band in the case of EhCaBP2 was diffuse suggesting that the level of phosphorylation and or glycosylation may also be different giving rise to a heterogeneous band.

In order to infer whether the two EhCaBPs bind to different sets of target proteins the *E. histolytica* lysate was first depleted of EhCaBP2-binding proteins by incubating with EhCaBP2-Sepharose. This was used to assay for both EhCaBP-dependent kinases. After depletion there was very low endogenous EhCaBP-dependent kinase activity. On addition of EhCaBP1 to depleted lysate the level of activation was found to be nearly at the same level as that obtained with normal lysate (Fig. 9, *lanes 3* and *5*). However, the level of activation of EhCaBP2-dependent kinase activity in depleted lysate was about 50% compared with that of 300% when normal lysate was used as a source of kinase (Fig. 9, *lanes 6* and *7*). The results suggest EhCaBP2-Sepharose could deplete specifically the kinase activated by it but not that activated by EhCaBP1.

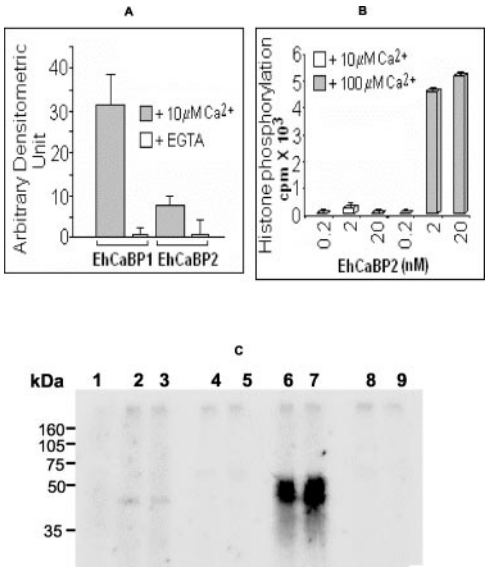

FIG. 8. **Stimulation of *E. histolytica* protein kinase by EhCaBP.** *E. histolytica* cell-free lysate (30 μg) was used as the source of the kinase and histone type III (40 μg) as the substrate. The amount of EhCaBP is 2 nM, unless otherwise indicated. The concentration of Ca^{2+} used in the experiments is indicated. EGTA was used at 500 μM. The assay was performed as described under "Experimental Procedures" using [γ-^{32}P]ATP as the phosphate donor. The amount of radioactivity incorporated into histone was determined either by PhosphorImager (Fuji BAS 800) analysis of 10% SDS-PAGE-separated phosphorylated products (*panel A)* or by scintillation counting of total trichloroacetic acid-precipitable proteins (*panel B*). Endogenous substrate phosphorylation by EhCaBP-dependent protein kinase. was performed with cell-free *E. histolytica* lysate (30 μg) and 2 nM each of EhCaBP1 (*lanes 2–5*) or EhCaBP2 (*lanes 6–9*) in the presence of 100 μM added Ca^{2+} (*lanes 2* and *3* and *lanes 6* and *7*) or 500 μM EGTA (*lanes 4* and *5* and *lanes 8* and *9*) as described earlier, except that histone was not added in the reaction mixture, *lane 1* did not have *Entamoeba* cell lysate but contained Ca^{2+} (*panel C*). The phosphorylated reaction mixes were visualized after separation on a 10% SDS-PAGE followed by autoradiography.

Therefore it appears that the two kinases may be distinctly different from each other.

Peptide C112 Binds EhCaBP2 Specifically—The two EhCaBPs were further distinguished on the basis of their binding to a dodecamer peptide, C112 (SMNLQTPGYKDG). This peptide was identified from a random dodecamer peptide phage display library by affinity purification using an EhCaBP-Sepharose column.[2] Phage-displayed peptides obtained from the above screen were tested for their differential binding to the two EhCaBPs. Binding was assayed using Ca^{2+}-dependent phage ELISA as described under "Experimental Procedures." The phage-displayed peptide C112 showed at least 5-fold higher Ca^{2+}-dependent binding to EhCaBP2 compared with EhCaBP1 (Fig. 10).

The extent of phage 112 binding to EhCaBP1 was negligible as the value was close to that obtained in the presence of EGTA. The parental M13 phage showed no significant binding. To check for nonspecific binding, bovine serum albumin was used for coating the ELISA plates instead of EhCaBP. The level of nonspecific binding was low (about 5% of specific binding). The binding of phage C112 to both the EhCaBPs was also checked by a real-time assay employing surface plasmon resonance. Using binding conditions as described under "Experimental Procedures," the affinity constant was found to be 14 μM for EhCaBP2 (Fig. 11). No binding was observed with EhCaBP1 under identical binding conditions, demonstrating the specificity of phage C112 for EhCaBP2.

[2] P. Chakrabarty, D. K. Sethi, K. J. Kaur, D. M. Salunke, S. Bhattacharya, and A. Bhattacharya, manuscript in preparation.

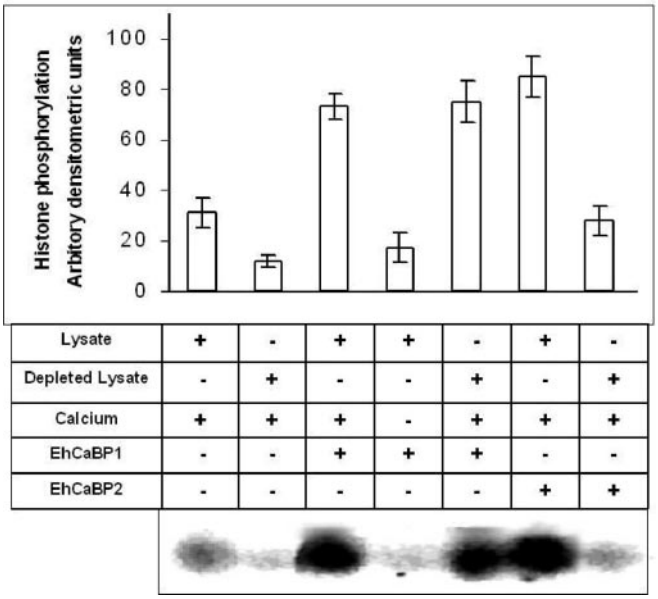

FIG. 9. **Depletion of EhCaBP2-dependent kinase activity by EhCaBP2-Sepharose.** *E. histolytica* cell-free lysate was incubated with EhCaBP2-Sepharose in the presence of 100 μM Ca^{2+} at 4 °C for 1 h, and the supernatant is referred to as a depleted source of protein kinase. Equal amounts (30 μg) of depleted lysate and normal undepleted lysate was used for checking the efficacy of either EhCaBP2- or EhCaBP1-dependent protein kinase activity. The respective EhCaBPs were used at 2 nM concentration. The amount of radioactivity incorporated into histone was determined by PhosphorImager analysis (Fuji BAS 800) of 10% SDS-PAGE-separated phosphorylated products. Representative bands obtained by autoradiographic exposure are shown.

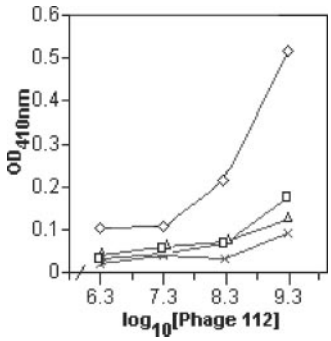

FIG. 10. **Binding of C112 phage to EhCaBP2 and EhCaBP1.** Indicated amounts of phage C112 were allowed to bind to 4 μg each of EhCaBP2 or EhCaBP1 immobilized on an ELISA plate. Binding assay was carried out in the presence of Ca^{2+} (2 mM) or EGTA (4 mM) as described under "Experimental Procedures." Bound phages were detected immunologically by incubating each well with HRPO-tagged anti M13 antibody. The plate-bound HRPO was detected with TMB substrate and absorbance recorded at 410 nm. -◇-, EhCaBP2/Ca^{2+}; -□-, EhCaBP2/EGTA; -△-, EhCaBP1/Ca^{2+} and ×, EhCaBP1/EGTA.

The binding of the synthetic peptide C112 to EhCaBP2 also blocked activation of endogenous kinase by EhCaBP2. In the presence of 100 pmole pC112, the inhibition was found to be about 85% of the EhCaBP2-dependent kinase activity (Fig. 12). No such inhibition was obtained when other 12-mer peptides, p12 and p61, were used in the kinase activation assay. This further demonstrates that the two EhCaBPs are functionally and structurally distinct. The sequence of C112 was used to search the Entamoeba genome data base at both Sanger Center and TIGR. None of the hit sequences obtained had a perfect match. The best match was 7 of 12 amino acids (data not shown).

DISCUSSION

EhCaBP1 is the first CaM-like calcium-binding protein that has been identified and characterized from *E. histolytica*. There

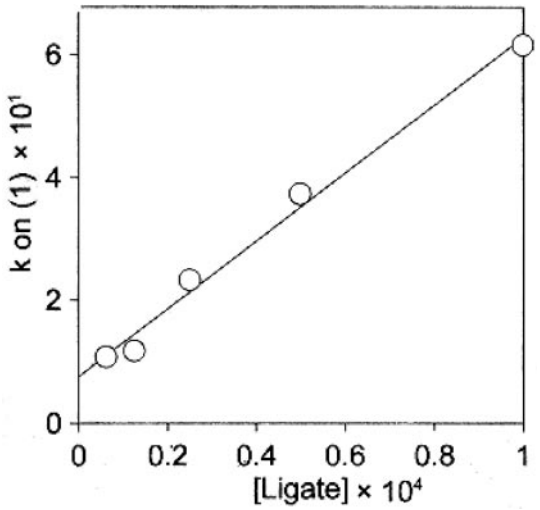

FIG. 11. **Surface plasmon resonance analysis of binding of phages to EhCaBP.** Biotinylated phages C112 (10^{10} phages) were allowed to bind uniformly to a streptavidin-coated cuvette. The cuvette was primed with the binding buffer (TBS containing 2 mM Ca^{2+}) to achieve a constant baseline. Different concentrations of EhCaBP2 protein prepared in the binding buffer were allowed to pass through the cuvette. Typical binding time allowed was 3–5 min. Dissociation was done using the binding buffer typically for 10 min. In certain cases, regeneration was done using TBS containing 4 mM EGTA until the baseline was achieved. Association and dissociation is represented as linear fit of the k_{on} with the protein concentration. The scales of the x- and y-axes are in molar (M) and s^{-1}, respectively.

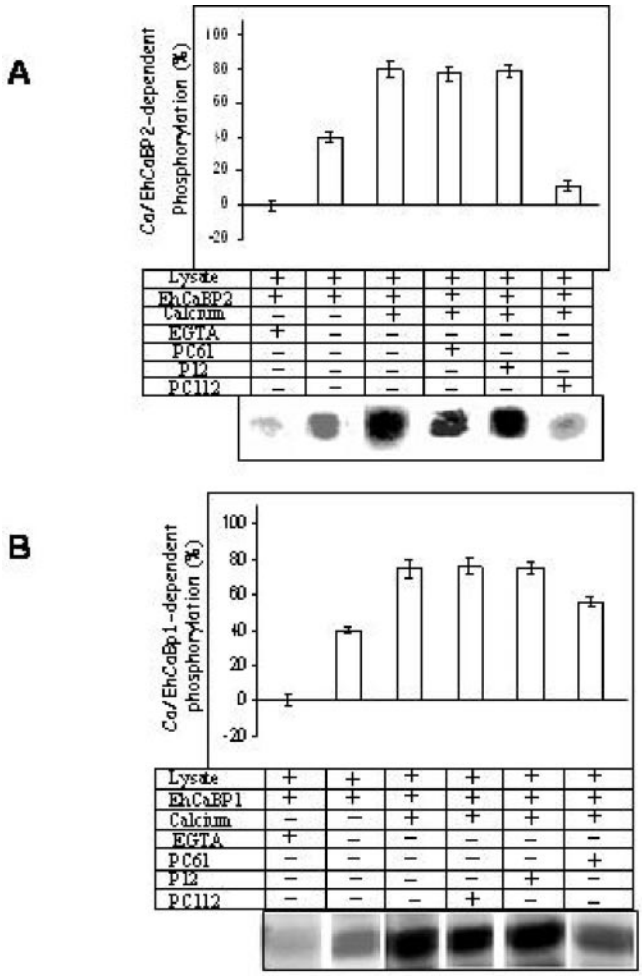

FIG. 12. **Inhibition of EhCaBP-dependent activation of protein kinase by peptide.** EhCaBP2- and EhCaBP1-stimulated protein kinase(s) was assayed using *E. histolytica* total cell-free lysate (30 μg) as the source of the kinase and histone type III (40 μg) as the substrate as described under "Experimental Procedures." The individual peptides were added to a final concentration of 100 pmol. The amount of Ca^{2+} used for EhCaBP2 and EhCaBP1-dependent kinase assays are 100 and 10 μM respectively. The amount of radioactivity incorporated into histone was determined by PhosphorImager analysis (Fuji BAS 800) of 10% SDS-PAGE-separated phosphorylated products. The corresponding autoradiographic signals are shown at the bottom of the *panels*. *Panel A*, EhCaBP2-dependent; *panel B*, EhCaBP1-dependent phosphorylation.

appears to be a CaM gene encoded in the genome of *E. histolytica* as inferred by sequence similarity and phylogenetic relationship (Fig. 2). The expression of this gene and functional analysis of the gene product has not been studied so far though work done several years ago indicated presence of CaM-like activity in this organism (19, 20, 23). EhCaBP was originally thought to be a form of primitive CaM. However, phylogenetic analysis and structure modeling studies described in this report and some of the experimental observations reported earlier, clearly show that the EhCaBPs are distinctly different from CaM (23). Both the EhCaBPs are phylogenetically close to each other and may have been derived by a duplication event.

Many CaBPs are known to be present in multiple copies (isoforms) in different organisms. Among these, CaM and CaM-like proteins have been studied quite extensively (41, 42, 43). One such CaM isoform, the epithelial cell protein CLP, has the same size and displays 85% sequence identity with CaM (41). Both CaM and CLP can activate CaM kinase II. However, CLP cannot activate four other CaM-dependent enzymes. In plants, soybean has four different CaM variants. Of these, SCaM4 shows the highest divergence at the level of amino acid sequence (44). Unlike SCaM1, SCaM4 did not activate NAD kinase, indicating subtle variations at the functional level that may be due to variations at the primary sequence level. Support for this comes from a study where a number of different single mutations in CaM (*e.g.* phenylalanine to alanine) altered its properties and the different mutants displayed distinctive functional defects (45). In addition, a number of single amino acid mutations in *Paramecium* CaM that did not alter growth properties, did however, display behavioral aberrations (46). Thus, changes in the protein interaction domain, without changing the rest of the protein can, in principle, alter the specificities of proteins. The human genome also contains a family of non-allelic CaM genes that are under selective pressure to encode identical proteins, while maintaining divergent nucleotide sequences of non-coding regions (43). Preserving multiple CaM genes with divergent non-coding sequences may be necessary in complex organisms to ensure that the many CaM-dependent processes occur with appropriate spatial and temporal control (43). Two or more non-allelic CaM or CaM-like genes have also been reported in *Xenopus* (47) and trypanosomes (48). Therefore it is not surprising that there are multiple forms of EhCaBP. The length and composition of the central linker region has been shown to be important for maintaining the functionality of CaM. Apart from binding to target peptide stretches, the linker has also been proposed to modulate metal ion binding and interdomain cooperativity (49). The major sequence divergence between the EhCaBPs, interestingly, spans this region, which suggests distinct functional roles for the two proteins. These molecules interacting with specific sets of target proteins may initiate different downstream pathways. This is evident from some of the results presented here that show different sets of binding proteins as revealed by affinity purification and subsequent analysis using MALDI-TOF mass spectrometry and the ability of the EhCaBP2 affinity matrix to deplete only EhCaBP2-dependent kinase activity but not EhCaBP1-dependent activity. Differences in the phosphorylation

patterns of the endogenous substrates by EhCaBP1 and EhCaBP2-dependent protein kinase(s) also indicate distinct functional pathways for these two closely related proteins.

The data presented here show that EhCaBP1 and EhCaBP2 are non-allelic variants with identical sizes and a high degree of identity at both nucleotide and amino acid sequence level. Since the upstream and downstream sequences flanking the coding regions are totally different, it is likely that the two EhCaBPs are located in different chromosomal regions. It is unlikely that there are other members of this family, since a search of the genome data base available as of now did not reveal any other isoforms.

Commensurate with the observed biochemical properties of the two proteins, the surface features in the two proteins show differences based on modeling studies. In general no difference was found in the regions that bind Ca^{2+} in these two proteins. The central linker region, connecting the two globular domains in CaM-like proteins has been a region of special interest for biochemists and structural biologists alike. Several site-directed mutageneses have been carried out in these proteins to understand the effect of length and composition of this linker on their individual functions (50, 51, 52). The flexible linker region between the two domains may contribute to the different juxtapositions of the Ca^{2+} binding domains. The presence of Gly^{63} and Gly^{67} in the linker region of EhCaBP1 was shown to be important for the function of EhCaBP1 as it provided flexibility to the region (26, 28). In one of the earlier studies on EhCaBP, these two Gly residues were mutated to Ala (53). Such mutations were found to impart rigidity to the flexible linker region. Circular dichroism and mass spectrometric techniques were also used to reveal that the mutant protein was weakened in its ability to bind Ca^{2+} and its target peptides (53), implying a possible role of these glycines in specific interactions with target peptides. In EhCaBP2, Gly^{63} and Gly^{67} have been changed to Ala^{63} and Glu^{67}, respectively. These changes along with charge differences are likely to affect the specificity of binding of the target proteins leading to altered functional properties. The identification of a peptide C112 that can bind EhCaBP2 selectively suggested distinctive specificity of target protein interaction by the two EhCaBPs. Though C112 has been identified from a pool of random peptides and not from a biological source, the selective binding indicates differences in the binding pocket between the two EhCaBPs. The inhibition of endogenous kinase showed that the binding of the peptide C112 to EhCaBP2 is biologically relevant as the binding data correlated with functional inhibition data. All these suggest that the two EhCaBPs are functionally distinct.

The signal transduction pathways involving both the EhCaBPs are currently being worked out. It will be interesting to see if there is any cross-talk or redundancy between the two pathways. To determine the cellular role of these two proteins, we are also planning to design specific inhibitors for both the EhCaBPs that will help elucidate the role of these two proteins *in vivo*.

Acknowledgments—We thank Prof. T. P. Singh and Dr. Sujata for MALDI-TOF and Dr. Dinkar Sahal for the use of the UV spectropolarimeter. Preliminary sequence data for *E. histolytica* used in this study were deposited regularly into the GSS division of GenBank™. The sequencing effort is part of the International Entamoeba Genome Sequencing Project and is supported by an award from NIAID, National Institutes of Health.

REFERENCES

1. Berridge, M. J., Lipp P., and Bootman, M. D. (2000) *Nat. Rev. Mol. Cell. Biol.* **1,** 11–21
2. Tsien, R. W., and Tsien, R. Y. (1990) *Annu. Rev. Cell Biol.* **6,** 715–760
3. Chin, D, and Means, A. R. (2000) *Trends Cell Biol.* **10,** 322–328
4. Scheibel, L. W. (1992) *Int. Rev. Cytol.* **134,** 165–242
5. Matsumoto, Y., Perry, G., Scheibel, L. W., and Aikawa, M. (1987) *Eur. J. Cell Biol.* **45,** 36–43
6. Johnson, J. G., Epstein, N., Shiroishi, T., and Miller, L. H. (1981) *J. Protozool.* **28,** 160–164
7. Pereira, C., Paveto, C., Espinosa, J., Alonso, G., Flawia, M. M., and Torres, H. N. (1997) *J. Eukaryot. Microbiol.* **44,** 155–156
8. Yakubu, M. A., Majumder, S., and Kierszenbaum, F. (1994) *Mol. Biochem. Parasitol.* **66,** 119–125
9. Modha, J., Roberts, M. C., Robertson, W. M., Sweetman, G., Powell, K. A., Kennedy, M. W., and Kusel, J. R. (1999) *Parasitology* **118,** 509–522
10. Bernal, R. M., Tovar, R., Santos, J. I., and Munoz, M. L. (1998) *Parasitol. Res.* **84,** 687–693
11. Meza, I. (2000) *Parasitol. Today* **16,** 23–28
12. Ravdin, J. I., Moreau, F., Sullivan, J. A., Petri, W. A., Jr., and Mandell, G. L. (1988) *Infect. Immunol.* **56,** 1505–1512
13. Weikel, C. S., Murphy, C. F., Orozco, E., and Ravdin, J. I. (1988) *Infect. Immun.* **56,** 1485–1491
14. Ganguly, A., and Lohia, A. (2001) *Mol. Biochem. Parasitol.* **112,** 277–285
15. Makioka, A., Kumagai, M., Ohtomo, H., Kobayashi, S., and Takeuchi, T. (2001) *Parasitol. Res.* **87,** 833–837
16. Nickel, R., Jacobs, T., Urban, B., Scholze, H., Bruhn, H., and Leippe, M. (2000) *FEBS Lett.* **486,** 112–116
17. Gilchrist, C. A., Holm, C. F., Hughes, M. A., Schaenman, J. M., Mann, B. J., and Petri, W. A., Jr. (2001) *J. Biol. Chem.* **276,** 11838–11843
18. Gilchrist, C. A., Leo, M., Line, C. G., Mann, B. J., and Petri, W. A., Jr. (2003) *J. Biol. Chem.* **278,** 4646–4653
19. Munoz, Mde L., Moreno, M. A., Perez-Garcia, J. N., Tovar, G. R., and Hernandez, V. I. (1991) *Mol. Microbiol.* **5,** 1707–1714
20. Munoz, M. L., O'Shea-Alvarez, M. S., Perez-Garcia, J., Weinbach, E. C., Moreno, M. A., de la Torre, M., Magos, M. A., and Tovar, R. (1992) *Comp. Biochem. Physiol. B.* **103,** 517–521
21. Prasad, J., Bhattacharya, S., and Bhattacharya, A. (1992) *Mol. Biochem. Parasitol.* **52,** 137–140
22. Prasad, J., Bhattacharya, S., and Bhattacharya, A. (1993) *Cell. Mol. Biol. Res.* **39,** 167–175
23. Yadava, N., Chandok, M. R., Prasad, J., Bhattacharya, S., Sopory, S. K., and Bhattacharya, A. (1997) *Mol. Biochem. Parasitol.* **84,** 69–82
24. Sahoo, N., Chakrabarty, P., Yadava, N., Bhattacharya, S., and Bhattacharya, A. (2000) *Arch. Med. Res.* **31,** S57–59
25. Sahoo, N., Bhattacharya, S., and Bhattacharya, A. (2003) *Mol. Biochem. Parasitol.* **126,** 281–284
26. Gopal, B., Suma, R., Murthy, M. R., Bhattacharya, A., and Bhattacharya, S. (1998) *Acta Crystallogr. Sect. D. Biol. Crystallogr.* **54,** 1442–1445
27. Sahu, S. C., Bhattacharya, A., Chary, K. V., and Govil, G. (1999) *FEBS Lett.* **459,** 51–56
28. Atreya, H. S., Sahu, S. C., Bhattacharya, A., Chary, K. V., and Govil, G. (2001) *Biochemistry* **40,** 14392–14403
29. Diamond, L. S., Harlow, D. R., and Cunnick, C. C. (1978) *Trans. R. Soc. Trop. Med. Hyg.* **72,** 431–432
30. Chandok, M. R., and Sopory, S. K. (1992) *Phytochemistry* **31,** 2255–2258
31. Gopal, B., Swaminathan, C. P., Bhattacharya, S., Bhattacharya, A., Murthy, M. R., and Surolia, A. (1997) *Biochemistry* **36,** 10910–10916
32. Smith, G. P., and Scott, J. K. (1993) *Methods Enzymol.* **217,** 228–257
33. Manivel, V., Bayiroglu, F., Siddiqui, Z., Salunke, D. M., and Rao, K. V. (2000) *J. Immunol.* **169,** 888–897
34. Sali, A., and Blundell, T. L. (1993) *J. Mol. Biol.* **234,** 779–815
35. Laskowski, R. A., Rullmannn, J. A., MacArthur, M. W., Kaptein, R., and Thornton, J. M. (1996) *J. Biomol. NMR.* **8,** 477–486
36. Barrow, C. J., Yasuda, A., Kenny, P. T. M., and Zagorski, M. G. (1992) *J. Mol. Biol.* **225,** 1075–1093
37. Smith, P. K., Krohn, R. I., Hermanson, G. T., Mallia, A. K., Gartner, F. H., Provenzano, M. D., Fujimoto, E. K., Goeke, N. M., Olson, B. J., and Klenk, D. C. (1985) *Anal. Biochem.* **150,** 76–85
38. Laemmli, U. K. (1970) *Nature* **227,** 680–685
39. Laskey, R. A., and Mills, A. D. (1975) *Eur. J. Biochem.* **56,** 335–341
40. Tanaka, T., Tanaka, M., and Mitsui, Y. (1997) *Biochem. Biophys. Res. Commun.* **236,** 611–615
41. Edman, C. F., George, S. E., Means, A. R., Schulman, H., and Yaswen, P. (1994) *Eur. J. Biochem.* **226,** 725–730
42. Stein, J. P., Munjaal, R. P., Lagace, L., Lai, E. C., O'Malley, B. W., and Means, A. R. (1983) *Proc. Natl. Acad. Sci. U. S. A.* **80,** 6485–6489
43. Toutenhoofd, S. L., and Strehler, E. E. (2000) *Cell Calcium* **28,** 83–96
44. Lee, S. H., Kim, J. C., Lee, M. S., Heo, W. D., Seo, H. Y., Yoon, H. W., Hong, J. C., Lee, S. Y., Bahk, J. D., Hwang, I., and Cho, M. J. (1995) *J. Biol. Chem.* **270,** 21806–21812
45. Ohya, Y., and Botstein, D. (1994) *Science* **263,** 963–966
46. Kink, J. A., Maley, M. E., Preston, R. R., Ling, K. Y., Wallen-Friedman, M. A., Saimi, Y., and Kung, C. (1990) *Cell* **62,** 165–174
47. Chien, Y. H., and Dawid, I. B. (1984) *Mol. Cell. Biol.* **4,** 507–513
48. Tschudi, C., Young, A. S., Ruben, L., Patton, C. L., and Richards, F. F. (1985) *Proc. Natl. Acad. Sci. U. S. A.* **82,** 3998–4002
49. Protasevich, I., Ranjbar, B., Lobachov, V., Makarov, A., Gilli, R., Briand, C., Laçtte, D., and Haiech, J. (1997) *Biochemistry* **36,** 2017–2024
50. van der Spoel, D., de Groot, B. L., Hayward, S., Berendsen, H. J., and Vogel HJ. (1996) *Protein Sci.* **5,** 2044–2053
51. VanBerkum, M. F., George, S. E., and Means, A. R. (1990) *J. Biol. Chem.* **265,** 3750–3756
52. Tabernero, L., Taylor, D. A., Chandross, R. J., VanBerkum, M. F., Means, A. R., Quiocho, F. A., and Sack, J. S. (1997) *Structure* **5,** 613–622
53. Moorthy, A. K. (2001) *Biophysical Studies on a Calcium-Binding Protein from Entamoeba histolytica and Its Mutants*. Ph.D. Thesis, Indian Institute of Science, Bangalore, India